ChemComm

Accepted Manuscript

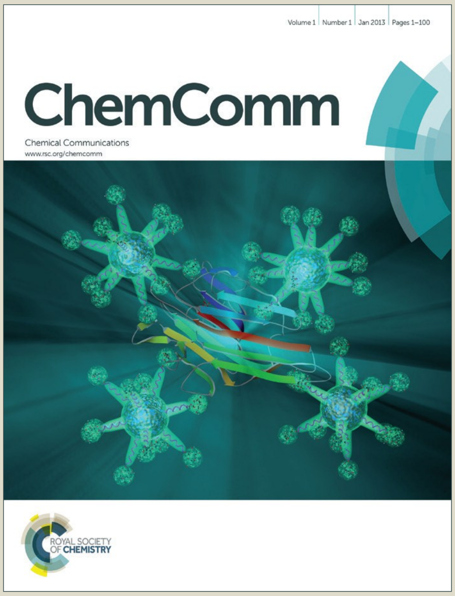

ROYAL SOCIETY OF CHEMISTRY

www.rsc.org/chemcomm

ROYAL SOCIETY OF CHEMISTRY

ChemComm

COMMUNICATION

Layered Gadolinium Hydroxides for Low-Temperature Magnetic Cooling

Received 00th January 20xx,
Accepted 00th January 20xx

DOI: 10.1039/x0xx00000x

Gonzalo Abellán,[a§] *†* Guillermo Mínguez Espallargas,[a§] Giulia Lorusso,[b] Marco Evangelisti,*[b] and Eugenio Coronado.*[a]

Layered gadolinium hydroxides have revealed to be excellent candidates for cryogenic magnetic refrigeration. These materials behave as pure 2D magnetic systems with a Heisenberg-Ising critical crossover, induced by dipolar interactions. This 2D character and the possibility offered by these materials to be delaminated open the possibility of rapid heat dissipation upon substrate deposition.

Two-dimensional (2D) materials are attracting an increasing interest in the last years.[1] Beyond graphene, layered metal hydroxides are promising candidates due to their chemical versatility and wide range of physical properties.[2–4] These materials present host-guest anion exchange properties allowing the intercalation of stimuli-responsive molecules that can be used for controlling their physical properties.[4–6] Moreover, they can be exfoliated into unilamellar nanosheets offering a plethora of different applications in sensors, energy storage and conversion, or magnetism, to name a few.[7] One of the newest families of compounds that have emerged are layered lanthanide hydroxides (LLHs), which can be described by the general formula of $Ln_2(OH)_5A{\cdot}nH_2O$, where A accounts for interlayer inorganic/organic anions such as Cl^-, NO_3^- or dodecylsulfate (DS^-).[8] LLHs have been recently postulated as excellent anion exchangers, precursors to unique functional oxides or optical phosphors.[9] With respect to their magnetic properties – despite their potential interest– the list of examples is very scarce and is almost limited to the study of a series of yttrium and dysprosium derivatives, showing a rich phenomenology including Single Ion Magnetic behaviour.[10,11]

However, the use of LLHs as low-temperature magnetic coolers has not yet been examined. In this sense, gadolinium-based molecular materials have been postulated as excellent alternatives to the well-established magnetic refrigerants at liquid-helium temperatures,[12] as they exhibit an enhanced magnetocaloric effect (MCE), *i.e.* the change of the magnetic entropy (ΔS_m) and related adiabatic temperature following a change of the applied magnetic field (ΔB).[13,14] In order to maximize the MCE, weak superexchange interactions in materials having a high density of magnetic centres are highly desired; along this front the use of geometric spin frustration, like 2D triangular AF lattices, gives rise to regions of high density of states.[15] Thus, the highly dense, almost hexagonal, 2D lattice of lanthanide cations bridged by hydroxide ligands present in LLHs, together with its low diamagnetic content, is a promising alternative to the list of extended materials with short bridges reported so far with MCE, which includes, among others, formates,[16,17] phosphates[18] and carbonates[19], being $[Gd(HCOO)(OAc)_2(H_2O)_2]$,[20] $[Gd(C_4O_4)(OH)(H_2O)_4]_n$,[21] $[Gd(C_2O_4)(H_2O)_3Cl]$,[22] and $[Gd(cit)(H_2O)]$,[23] the only 2D structures. Importantly, the ability of LLHs to be delaminated[3] provide additional advantages for rapid heat dissipation, as the delaminated material could be placed on a substrate thus enhancing heat transportation.[24,25] Herein, we report the MCE of two Gd^{3+}-based layered hydroxides, namely pristine $Gd_2(OH)_5Cl{\cdot}1.5H_2O$ (**LLH-1**), and the Gd hydroxide intercalated with dodecyl sulfate $Gd_2(OH)_5DS{\cdot}nH_2O$ (**LLH-2**, DS^- = $C_{12}H_{25}SO_3^-$). Their large MCE is quantitatively superior to almost all the best Gd-based clusters, and is similar to that recently reported for extended frameworks. Given the excellent processability exhibited by these compounds and their large-scale production, the Gd-LLHs represent an avenue worth to being explored.

The synthesis of **LLH-1** has been developed following the homogeneous alkalization route using NaCl as the anion source (see Supporting Information for additional experimental details and further characterization).[8] The intercalation of DS^- was performed using the approach reported by Hu and co-workers.[26] Figure 1 shows the crystalline structure of the layers,[27] which contains three crystallographic distinct sites for the gadolinium with two different environments, one 8-fold coordinated unit in a dodecahedron environment, $[Gd(OH)_7(H_2O)]$, and two 9-fold coordinated units with a monocapped square antiprism geometry, $[Gd(OH)_8(H_2O)]$.

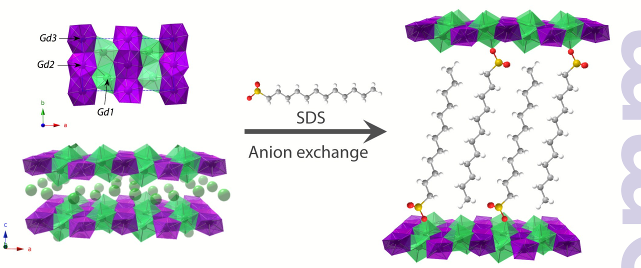

Fig. 1 $Gd_2(OH)_5Cl{\cdot}1.5H_2O$ (**LLH-1**) crystal structure viewed along the *c*-axis (top) and *b*-axis (bottom). Schematic representation of the dodecyl sulphate intercalation ($C_{12}H_{25}SO_3^-$) giving rise to **LLH-2** exhibiting an expanded interlayer space. The 8-coordinated dodecahedra and 9-coordinated monocapped square antiprisms are highlighted in green and purple colours, respectively.

The crystal structure is composed by edge-sharing polyhedra, with the hydroxyl groups acting as μ_3-bridge between the Gd centers yielding very short Gd···Gd distances (3.957, 3.944 and 3.662 Å). The powder X-ray diffraction (PXRD) pattern of **LLH-1** shows sharp and intense peaks denoting a high crystallinity (Figure S4). In this case, the sheets are separated by Cl^- anions, giving an interlayer distance of *ca*. 8.4 Å. The PXRD pattern of **LLH-2** presents a shift of the diffraction peaks towards lower 2-ϴ values resulting in an increased interlayer space of *ca*. 2.5 nm, indicative of an interdigitated disposition of the DS$^-$ molecules within the interlamellar space.

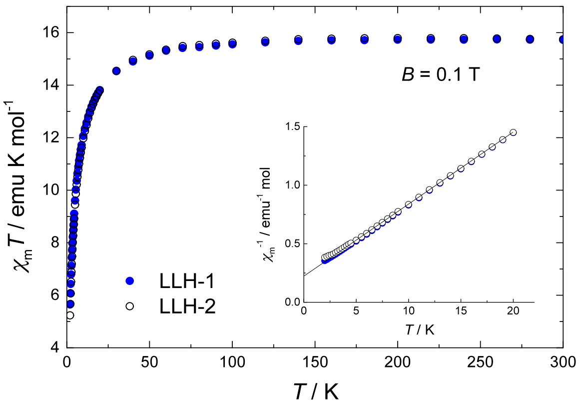

Fig. 2 Temperature-dependencies of the magnetic susceptibility product, $\chi_m T$ at 2–300 K with a dc field of 0.1 T for **LLH-1** and **LLH-2**, denoting predominant antiferromagnetic interactions. Inset: Same set of data as χ_m^{-1} vs. T for $T < 20$ K, together with the fit to the Curie-Weiss law (solid line).

The morphology of the as-synthesized materials has been studied by scanning electron microscopy, revealing a homogeneous distribution of anisotropic platelet-like particles of less than one micron in lateral dimensions before and after the intercalation process (Figures S5 and S6). Exfoliation of **LLH-2** produces nanosheets of *ca*. 3 nm thickness, as estimated by AFM (Figure S7), which correspond to mono- or bi-layers, as previously described.[26,28]

Figure 2 depicts the variable temperature magnetic susceptibility measurements above 2 K of both samples in an applied dc field of 0.1 T. At room temperature, the $\chi_m T$ value is 15.7 emu·mol^{-1}·K, which is in good agreement with the spin-only value expected for two uncoupled Gd^{3+} centres (2×7.875 emu·mol^{-1}·K). Upon cooling below 100 K, $\chi_m T$ decreases significantly, denoting dominant antiferromagnetic interactions, likely extending over the *ab* planes. No clear differences could be observed between the compact **LLH-1** and the expanded **LLH-2** system, except for the lowest temperatures, $T < 3$ K (see Figure 2). As shown by the solid line, the data can be fitted between 3 K and 300 K by a Curie-Weiss law $\chi_m = C/(T - \Theta_{CW})$, where $C = g^2\mu_B{}^2 s(s+1)/(3k_B)$, for $s = 7/2$, $g = 2.0$ and $\Theta_{CW} = 3.1$ K. Using the mean-field expression for the Curie-Weiss temperature $\Theta_{CW} = 2z|J|s(s+1)/(3k_B)$, where z is the number of nearest neighbours, we find the estimate $zJ/k_B \approx -0.3$ K for the antiferromagnetic interaction strength within the *ab* planes, for both compounds. Magnetization (M) versus applied field data, collected for the 2 K < T < 10 K range and applied fields up to 5 T corroborates the paramagnetic susceptibility of both compounds (Figure S8).

Specific heat (c) measurements down to *ca*. 0.3 K reveal differences between the two compounds (Figures 3 and 4). At the higher temperatures, c is dominated by a nonmagnetic contribution arising from thermal vibrations of the lattice, which can be modelled by the Debye-Einstein model.[29] The lattice specific heat simplifies to a $c/R = aT^3$ dependence at the lowest temperatures, where R is the gas constant and $a = 1.5\times10^{-4}$ K^{-3} and 1.0×10^{-3} K^{-3} for **LLH-1** and **LLH-2**, respectively. This difference indicates a stiffer structure than **LLH-1**, as indeed expected.

At low temperatures and large applied fields, the magnetic contribution to the specific heat (c_m), as resulting from subtracting the lattice contribution to the total specific heat, exhibits the typical Schottky-type anomalies originated by the splitting of the $s = 7/2$ multiplet (Figure 3). For zero-applied field, the specific heat is characterized by a lambda-like peak denoting the occurrence of a magnetic phase transition at $T_N^{(1)} = 1.3$ K for **LLH-1** and a slightly lower $T_N^{(2)} = 1.2$ K for **LLH-2** (Figure 4). Since no phase transition can occur at nonzero temperature for isotropic 2D magnetic lattices, the observed T_N's could either be ascribed to an Ising-type anisotropy or 3D coupling.[30] We disregard the latter option since the structure of the compounds should favour *stronger* intralayer magnetic fluctuations that give rise to a broad bump in c for temperatures higher than that of the phase transition, induced by the *weaker* interlayer coupling, in clear disagreement with the measurements (Figure 4). Therefore, one has to conclude that an anisotropy crossover from Heisenberg to Ising takes place in the critical temperature region. We argue that this behaviour can be understood in terms of a dipolar anisotropy. Let us first hypothetically assume that no superexchange interactions are present. If so, then the dipolar energy is minimized when all spins align ferromagnetically on the *ab* planes.[31] Let us next add intralayer antiferromagnetic superexchange interactions significantly stronger than the dipolar ones. If so, then aligning the antiferromagnetically-coupled spins on the *ab* planes would no longer be energetically favourable. In this case, neglecting any source of geometric spin frustration, spins would preferably point perpendicularly to the layers, *i.e.*, along the c axis. Using the structure of **LLH-1** and associating each Gd^{3+} spin to a point-dipole with $s = 7/2$, we have calculated the dipolar energies (E_d) for both the aforementioned magnetic structures. For **LLH-1**, we obtain $E_d^{(F//ab)} = -0.7$ K and $E_d^{(AF//c)} = -0.2$ K, respectively. For **LLH-2**, we repeat the calculation using the same structure except for the distance between the layers, which we increase up to the experimentally determined value of 2.5 nm. We thus obtain significantly weaker energies, *i.e.*, $E_d^{(F//ab)} = -0.4$ K and $E_d^{(AF//c)} = -0.1$ K, respectively. Next, from the difference in dipolar energy for the

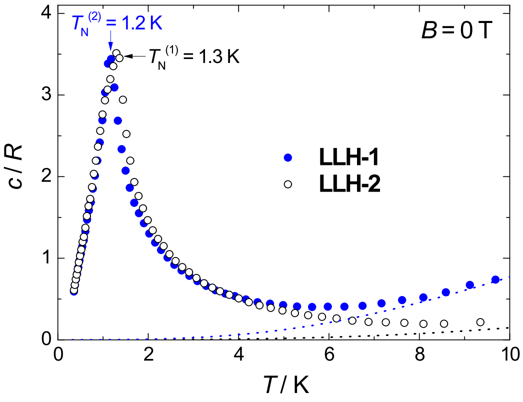

Fig. 3 Temperature-dependencies of the zero-applied-field specific heat, for **LLH-1** and **LLH-2**, normalized to the gas constant (R). The peaks at $T_N^{(1)}$ = 1.3 K and $T_N^{(2)}$ = 1.2 K denote the transition to a long-range magnetically ordered state for **LLH-1** and **LLH-2**, respectively. The dotted lines represent the Debye-Einstein model for the lattice specific heat.

two orientations considered, we obtain the anisotropy field B_a = 0.10 T and 0.06 T for **LLH-1** and **LLH-2**, respectively. Note that we likely overestimate these values since a full collinear magnetic ordering is hindered by the geometric spin frustration on the *ab* planes. The so-obtained B_a values are significantly smaller than the exchange field $B_{ex} = 2z|J|s/(g\mu_B) \approx 1.6$ T, thus yielding $(B_a/B_{ex}) \approx 6\times10^{-2}$ and 4×10^{-2} for **LLH-1** and **LLH-2**, respectively. A comparable $B_a/B_{ex}) \approx 8\times10^{-2}$ is found in the 2D antiferromagnet $GdBa_2Cu_3O_{6+x}$, whose magnetic ordering mechanism closely resembles the one reported here.[32] As for $GdBa_2Cu_3O_{6+x}$ and other 2D antiferromagnets,[29,31] the ordering temperature depends very weakly on (B_a/B_{ex}),[33] in agreement with the measured T_N's for **LLH-1** and **LLH-2**.

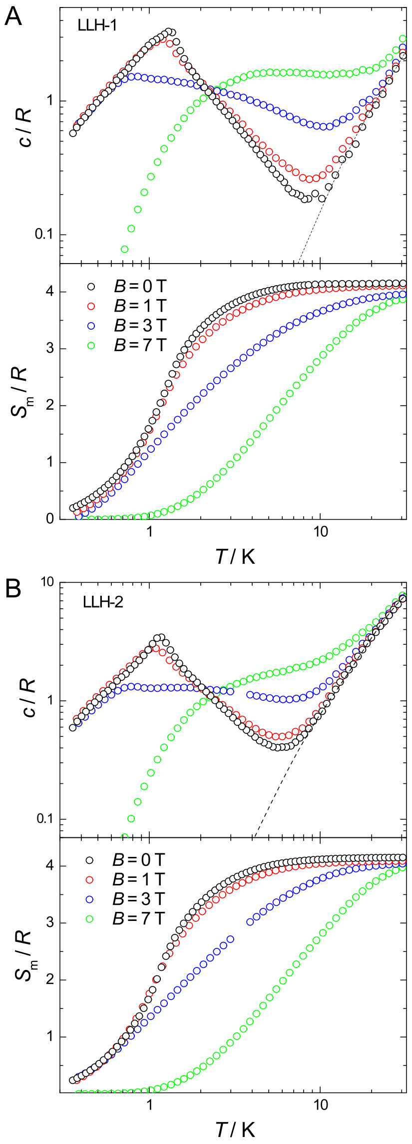

Fig. 4 Temperature-dependencies of the molar specific heat and magnetic entropy for **LLH-1** (A) and **LLH-2** (B). Top: Temperature-dependencies of the specific heat, *c*, normalized to the gas constant (*R*) and measured for several applied magnetic fields, as labelled. The dotted line represents the Debye-Einstein model for the lattice specific heat. Bottom: Corresponding temperature-dependencies of the magnetic entropy, S_m, as obtained from the magnetic contribution to the specific heat. S_m saturates to the maximum entropy value per mole involved corresponding to two Gd^{3+} ions, *i.e.*, $2\times R\ln(2s_{Gd}+1) \approx 4.2R$.

Finally, we evaluate the MCE for both compounds by determin , the magnetic entropy change, $-\Delta S_m$, as a function of temperatur and for selected applied field changes, ΔB, following well-know data-processing procedures.[13] From the magnetic entropy data in Figure 3, we straightforwardly obtain the $-\Delta S_m(T,\Delta B)$ curves depicted in Figure 5. As can be there seen, the curves for ΔB = 1 and 3 T agree nicely with the ones calculated by applying th Maxwell relation $\Delta S_m = \int \partial M/\partial T dB$ to the magnetization data Figure S8, thus validating the two independent derivations employed. Note that, not unexpectedly, the $-\Delta S_m(T,\Delta B)$ curves f r both compounds overlap one another for the same set of *T* and ΔB values (Figure 5). Clearly, the intralayer superexchange interaction (which has the same strength for both compounds) is the ma responsible for the MCE data showed in Figure 5, since the wea dipolar interactions become significant only at the lowest *B* and *i.e.*, well below the temperatures that correspond to the maxima of $-\Delta S_m(T,\Delta B)$. For ΔB = 1 T, the MCE is rather small and clear hindered by the intralayer antiferromagnetic interactions. Higher fields promote a larger magnetic decoupling and the dependence of $-\Delta S_m$ increases notably (Figure 5). For the larg field change ΔB = 7 T, $-\Delta S_m$ reaches 3.0*R* at *T* = 2.2 K, whic smaller than the maximum entropy value per mole involved, *i.e.*, $2\times R\ln(2s+1) \approx 4.2R$. Notwithstanding ΔB = 7 T is not yet suffic for achieving the full magnetocaloric potential, the measure maximum entropy change is significantly large, as readily evident by expressing $-\Delta S_m$ in the most common choice of units, *i.e.*, $-\Delta S_m$ =

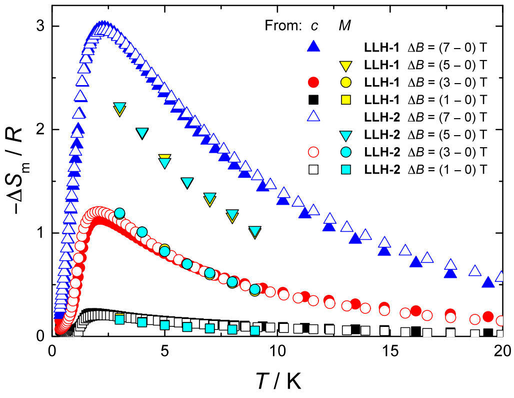

Fig. 5 Temperature-dependencies of the magnetic entropy change, $-\Delta S$ normalized to the gas constant *R*, obtained from magnetization (*M*) ar specific heat (c) data, for the applied-field changes ΔB and compounds **LL -1** and **LLH-2**, as labelled.

51.9 and 42.0 J kg^{-1} K^{-1} at *T* = 2.2 K and ΔB = 7 T for **LLH-1** and **LL 2**, respectively. This results from the high magnetic/non-magnet ratio (relatively low molecular mass) of both compounds. **LLH-1** neatly surpasses the values reported for 2D complexes so far,[23] and compares favourably with the recent reported records.[17,18]

In summary, we reported for the very first time the cryogen MCE of a layered lanthanide hydroxide, exhibiting significant large values for the ≈ (1.5 – 7) K temperature range. The interlayer dipolar interactions have been evaluated b hybridization of the pristine material with DS^- molecules. Magnetic ordering of the Gd^{3+} ions develops in the form of 2D Heisenberg-Ising crossover behaviour near the temperature, as induced by the dipolar interactions. The intrinsic 2D spin frustrated topology could be considered as an extension of the 0D heptametallic gadolinium molecule,[15] serving as an ideal example of extended triangular AF nets where dipolar and exchange contributions compete. Furthermore, as these layered materials can be exfoliated into unilamellar nanosheets[3], produced in large scale,[8] and processed into complex architectures,[34] they can be proposed as active elements for on-chip magnetic microrefrigerators[25] and excellent alternatives to the existing commercial low-temperature refrigerants.

We are grateful to the EU (ERC Advanced Grant SPINMOL), the Spanish MINECO (Projects MAT-2014-56143-R, CTQ-2014-59209-P and FEDER-MAT2012-38318-C03), and the Generalitat Valenciana (Prometeo Program and ISIC-Nano). Support from INNCIDE program through Vicerectorat d'Investigació i Política Científica of the University of Valencia is also acknowledged. G. A. thanks the EU for a Marie Curie Fellowship (FP7/2013-IEF-627386). G.M.E. thanks the Spanish MINECO for a Ramón y Cajal Fellowship.

Notes and references

[a] *Instituto de Ciencia Molecular (ICMol), Universidad de Valencia, 46980, Valencia, Spain. E-mail: eugenio.coronado@uv.es.*
[b] *Instituto de Ciencia de Materiales de Aragón (ICMA) and Departamento de Física de la Materia Condensada, CSIC–Universidad de Zaragoza, Pedro Cerbuna 12, 50009 Zaragoza, Spain. Email: evange@unizar.es.*

§ These authors contributed equally to this work

† Current address: Department of Chemistry and Pharmacy and Institute of Advanced Materials and Processes (ZMP), University Erlangen-Nürnberg, Henkestr. 42, 91054 Erlangen and Dr.-Mack Str. 81, 90762 Fürth, Germany.

Electronic Supplementary Information (ESI) available: Experimental details, PXRD analysis, SEM experiments, and isothermal magnetization curves. See DOI: 10.1039/c000000x/

1 A. C. Ferrari, F. Bonaccorso, V. Fal'ko, K. S. Novoselov, S. Roche, P. Bøggild, S. Borini, F. H. L. Koppens, V. Palermo, N. Pugno, J. A. Garrido, R. Sordan, A. Bianco, L. Ballerini, M. Prato, E. Lidorikis, J. Kivioja, C. Marinelli, T. Ryhänen, A. Morpurgo, J. N. Coleman, V. Nicolosi, L. Colombo, A. Fert, M. Garcia-Hernandez, A. Bachtold, G. F. Schneider, F. Guinea, C. Dekker, M. Barbone, Z. Sun, C. Galiotis, A. N. Grigorenko, G. Konstantatos, A. Kis, M. Katsnelson, L. Vandersypen, A. Loiseau, V. Morandi, D. Neumaier, E. Treossi, V. Pellegrini, M. Polini, A. Tredicucci, G. M. Williams, B. H. Hong, J.-H. Ahn, J. M. Kim, H. Zirath, B. J. van Wees, H. van der Zant, L. Occhipinti, A. D. Matteo, I. A. Kinloch, T. Seyller, E. Quesnel, X. Feng, K. Teo, N. Rupesinghe, P. Hakonen, S. R. T. Neil, Q. Tannock, T. Löfwander and J. Kinaret, *Nanoscale*, 2015, **7**, 4598–4810.
2 Q. Wang and D. O'Hare, *Chem. Rev.*, 2012, **112**, 4124–4155.
3 R. Ma and T. Sasaki, *Acc. Chem. Res.*, 2015, **48**, 136–143.
4 G. Abellán, C. Martí-Gastaldo, A. Ribera and E. Coronado, *Acc. Chem. Res.*, 2015, **48**, 1601−1611.
5 G. Abellán, E. Coronado, C. Martí-Gastaldo, A. Ribera, J. L. Jordá and H. García, *Adv. Mater.*, 2014, **26**, 4156–4162.
6 G. Abellán, J. L. Jordá, P. Atienzar, M. Varela, M. Jaafar, J. Gómez-Herrero, F. Zamora, A. Ribera, H. García and E. Coronado, *Chem Sci*, 2015, **6**, 1949–1958.
7 R. Ma and T. Sasaki, *Adv. Mater.*, 2010, **22**, 5082–5104.
8 F. Geng, Y. Matsushita, R. Ma, H. Xin, M. Tanaka, F. Izumi, N. Iyi and T. Sasaki, *J. Am. Chem. Soc.*, 2008, **130**, 16344–16350.
9 a) L.J McIntyre, L.K. Jackson and A.M. Fogg, *Chem. Mater.*, 2008, **20**, 335–340. b) J. Liang, R. Ma and T. Sasaki, *Dalton Trans.*, 2014, **43**, 10355–10364.
10 B. Monteiro, C. C. L. Pereira, J. T. Coutinho, L. C. J. Pereira, J. Marçalo and M. Almeida, *Eur. J. Inorg. Chem.*, 2013, **2013**, 5059–5063.
11 B. Monteiro, J. T. Coutinho, C. C. L. Pereira, L. C. J. Pereira, J. Marçalo, M. Almeida, J. J. Baldoví, E. Coronado and A. Gaita-Ariño, *Inorg. Chem.*, 2015, **54**, 1949–1957.
12 J. W. Sharples and D. Collison, *Polyhedron*, 2013, **54**, 91–103.
13 M. Evangelisti and E. K. Brechin, *Dalton Trans.*, 2010, **39**, 4672–4676.
14 J.-L. Liu, Y.-C. Chen, F.-S. Guo and M.-L. Tong, *Coord. Chem. Rev.*, 2014, **281**, 26–49.
15 J. W. Sharples, D. Collison, E. J. L. McInnes, J. Schnack, E. Palacios and M. Evangelisti, *Nat. Commun.*, 2014, **5**.
16 R. Sibille, T. Mazet, B. Malaman and M. François, *Chem. – Eur. J.*, 2012, **18**, 12970–12973.
17 G. Lorusso, J. W. Sharples, E. Palacios, O. Roubeau, E. K. Brechin, R. Sessoli, A. Rossin, F. Tuna, E. J. L. McInnes, D. Collison and M. Evangelisti, *Adv. Mater.*, 2013, **25**, 4653–4656.
18 E. Palacios, J. A. Rodríguez-Velamazán, M. Evangelisti, G. J. McIntyre, G. Lorusso, D. Visser, L. J. de Jongh and L. A. Boatner, *Phys. Rev. B*, 2014, **90**, 214423.
19 Y.-C. Chen, L. Qin, Z.-S. Meng, D.-F. Yang, C. Wu, Z. Fu, Y.-Z. Zheng, J.-L. Liu, R. Tarasenko, M. Orendáč, J. Prokleška, V. Sechovský and M.-L. Tong, *J. Mater. Chem. A*, 2014, **2**, 9851–9858.
20 G. Lorusso, M. A. Palacios, G. S. Nichol, E. K. Brechin, O. Roubeau and M. Evangelisti, *Chem. Commun.*, 2012, **48**, 7592–7594.
21 S. Biswas, A. Adhikary, S. Goswami and S. Konar, *Dalton Trans.*, 2013, **42**, 13331–13334.
22 Y. Meng, Y.-C. Chen, Z.-M. Zhang, Z.-J. Lin and M.-L. Tong, *Inorg. Chem.*, 2014, **53**, 9052–9057.
23 S.-J. Liu, C.-C. Xie, J.-M. Jia, J.-P. Zhao, S.-D. Han, Y. Cui, Y. Li and X.-H. Bu, *Chem. – Asian J.*, 2014, **9**, 1116–1122.
24 V. Corradini, A. Ghirri, A. Candini, R. Biagi, U. del Pennino, G. Dotti, E. Otero, F. Choueikani, R. J. Blagg, E. J. L. McInnes and M. Affronte, *Adv. Mater.*, 2013, **25**, 2816–2820.
25 G. Lorusso, M. Jenkins, P. González-Monje, A. Arauzo, J. Sesé, D. Ruiz-Molina, O. Roubeau and M. Evangelisti, *Adv. Mater.*, 2013, **25**, 2984–2988.
26 L. Hu, R. Ma, T. C. Ozawa and T. Sasaki, *Chem. – Asian J.*, 2010, **5**, 248–251.
27 F. Geng, R. Ma and T. Sasaki, *Acc. Chem. Res.*, 2010, **43**, 1177–1185.
28 B.-I. Lee, K. S. Lee, J.H. Lee, I. S. Lee and S.-H. Byeon, *Dalton Trans.* 2009, 2490–2495.
29 M. Evangelisti, F. Luis, L. J. de Jongh and M. Affronte, *J. Mater. Chem.*, 2006, **16**, 2534–2549.
30 L. J. D. Jongh and A. R. Miedema, *Adv. Phys.*, 2001, **50**, 947–1170.
31 L. J. de Jongh, *Magnetic Properties of Layered Transition Metal Compounds*, Springer Science & Business Media, 1990.
32 K. Nehrke and M. W. Pieper, *Phys. Rev. B*, 1995, **51**, 12618–12626.
33 K. Binder and D. P. Landau, *Phys. Rev. B*, 1976, **13**, 1140–1155.
34 B.-I. Lee, E. Lee and S.-H. Byeon, *Adv. Funct. Mater.*, 2012, **22**, 3562–3569.